23 MHz widely wavelength-tunable L-band dissipative soliton from an all-fiber Er-doped laser

QIANQIAN HUANG,[1] CHUANHANG ZOU,[1] CHENGBO MOU,[1,*] XI GUO,[2] ZHIJUN YAN,[2] KAIMING ZHOU,[3] AND LIN ZHANG[3]

[1]*Key Laboratory of Specialty Fiber Optics and Optical Access Networks, Shanghai Institute for Advanced Communication and Data Science, Joint International Research Laboratory of Specialty Fiber Optics and Advanced Communication, Shanghai University, Shanghai 200444, China*
[2]*School of Optical and Electronic Information, National Engineering Laboratory for Next Generation Internet Access System Huazhong University of Science and Technology, Wuhan, China*
[3]*Aston Institute of Photonic Technologies (AIPT), Aston University, Birmingham, B4 7ET, United Kingdom*
* mouc1@shu.edu.cn

Abstract: Via careful choice of Er-doped fiber length in the cavity, a widely wavelength-tunable L-band dissipative soliton all-fiber Er-doped laser incorporating a L-band optimized polarizing fiber grating device is experimentally demonstrated. The laser delivers 15.38 ps dissipative soliton pulses centered at 1597.34 nm with 3 dB bandwidth of 34.6 nm under 622 mW pump power. The pulse repetition rate is 23 MHz. After using single mode fiber at external cavity, the pulse duration is compressed to 772 fs. With nonlinear polarization rotation-based intracavity comb filter, the central wavelength of the generated dissipative soliton can be tuned from 1567 nm to 1606 nm with a spectral tuning range of 39 nm, which, to the best of our knowledge, is the widest tuning range yet reported for a dissipative soliton fiber laser working in communication band.

1. Introduction

Recently, wavelength-tunable mode locked fiber laser has emerged as a candidate light seed for diverse applications, e.g. material processing [1], fiber senor [2], spectroscopy [3], optical signal processing [4] as well as optical communication [5]. Especially, from the perspective of applications in term of optical communication, the L-band (1565 nm~1625 nm) is playing a great role at present due to the demanding requirement of communication capacity [6]. Therefore, investigation on L-band mode locked fiber laser with spectral tunability is significantly interesting.

To achieve tuning of center wavelength in a mode locked fiber laser, generally speaking, tunable spectral filters have to be involved such as Mach-Zehnder interferometers [7], Fabry-Perot interferometer [8], chirped fiber Bragg grating [9], few mode fiber filter [10], W-shape long period grating [11], polarization-maintaining (PM) fiber-based birefringence filter [12] *etc*. However, the formation of these filters requires additional components in the cavity, which complicated the laser configuration. Fortunately, it has been pointed out that taking advantage of the intracavity polarizer and intrinsic fiber birefringence, nonlinear polarization rotation (NPR) can induce wavelength-dependent loss and form an intracavity fiber birefringence comb filter [13]. Such type of filter possesses inherent merits of simplicity and flexibility. More importantly, NPR is also deemed as an effective mode locking technique in virtue of the advantages of ultra-short response time and high modulation depth [14,15], thereby finding an extensive utilization in spectral-tunable mode locked fiber lasers [16–20]. J. L. Luo *et al* experimentally demonstrated an NPR-based wavelength-tunable L-band mode locked fiber laser [18]. Despite 28 nm spectral tuning range was realized, the obtained pulse

showed conventional soliton (CS) exhibiting low pulse energy, which is the essential feature of CS [21]. Furthermore, CS tends to split when pump power increases further owing to the soliton energy quantization effect [22] and peak power limitation effect [23]. Comparatively, the dissipative soliton (DS) can resolve the aforementioned limitations of CS since it features higher pulse energy and resist to break on account of the presence of giant pulse chirp [24].

D. D. Han *et al* experimentally investigated a tunable DS fiber laser based on hybrid technique using both single walled carbon nanotubes (SWCNTs) and NPR [19]. D. Yan *et al* observed the spectral tunable DSs with NPR mechanism [20]. Despite the demonstration of about 20 nm tuning range in the aforementioned reports, these types of lasers incorporate Er-doped fiber (EDF) as long as a few tens of meters. It is appreciated that an extended length of EDF would provide enough gain at L band due to the intra-band absorption. Nevertheless, such excessively long EDF not only increases the cost, but also makes the excessive cavity length, resulting in instability and complexity of the laser. Furthermore, some studies have demonstrated that the laser wavelength-tuning range shows great dependency on the length of EDF [25,26]. Thus, in order to achieve stable and widely wavelength-tunable operation in a fiber laser, it is of particular necessary to optimize the properties of EDF.

In this contribution, we experimentally investigate a widely wavelength-tunable L-band DS all-fiber Er-doped laser by optimizing the length of EDF. A L-band optimized polarizing element acted by a 45°titlted fiber grating (45°TFG) with 48.4 dB peak polarization dependent loss (PDL) at 1593 nm and the intracavity fiber birefringence are combined together to implement NPR technique, which simultaneously realize mode locking and fiber birefringence comb filter. Under 622 mW pump power, 15.38 ps DS is obtained with a central wavelength of 1597.34 nm and 34.6 nm 3dB bandwidth. Worthy of mentioning, it is the first demonstration of L-band DS fiber laser using an operation band optimized polarizing fiber grating. When a suitable length of SMF is incorporated out of cavity, the pulse duration is decreased to 772 fs. In addition, aided by intracavity fiber birefringence comb filter, the laser permits the generation of spectral tunable DSs ranging from 1567 nm to 1606 nm, i.e. 39 nm tuning range. To the best of our knowledge, this is a record wide tunability with C + L band DS fiber laser. Noted that the cavity length is only 9.05 m, which is much shorter than those referred in [18–20]. Also, our experiment results demonstrate that the long cavity length, namely representing large intracavity birefringence, is not the key factor of realizing widely wavelength-tuning range in fiber laser incorporating the NPR-induced filter. We believe that such widely wavelength-tunable L-band DS all-fiber laser with femtosecond pulse duration as well as relatively short cavity length can be considered as an effective light source to fulfill the requirements of manifold applications.

2. Characterization of polarizing fiber grating and laser configuration

As proved in previous studies [27–29], the 45°TFG have been considered as an effective in-fiber polarizer, because it can compel *s*-light out of grating while allow *p*-light pass with low loss. In order to characterize the features of 45°TFG, a vector optical analyzer incorporating a tunable laser with the operating range between 1525 nm to 1610 nm is employed. The PDL measurement result is plotted in Fig. 1(a), and the corresponding maximum loss and minimum loss are illustrated in Fig. 1(b), which are measured at two orthogonal polarization states. To alternate the PDL response of the 45°TFG, we simply tune the tilted angle of the phase mask by rotating a goniometer by less than 1°. Clearly, compared to former works [27–29], the peak of PDL profile locates at 1593 nm is 48.4 dB, which means that the 45°TFG is designed to operate exclusively at L-band and can function as an effective polarizer to achieve NPR mechanism at the chosen region [30]. Also, one can find that there are notable spectral ripples arising from the mismatching refraction index between cladding and radiation mode, which technically do not affect the performances of the laser. It can be removed by immersing it into refraction index matching gel. Correspondingly, the measured maximum loss and minimum loss of the grating are −1.9 dB, −50.3 dB respectively. This confirms the

low insertion loss feature of the device. Furthermore, the transmission spectrum of the 45° TFG is shown in Fig. 1(c). There is a narrow dip in 1581 nm indicating the existence of second order Bragg resonance, which don't affect the performances of the laser neither. Notably, the PDL in a broad range remains obviously above 30 dB, revealing an attractive feature of broadband operation.
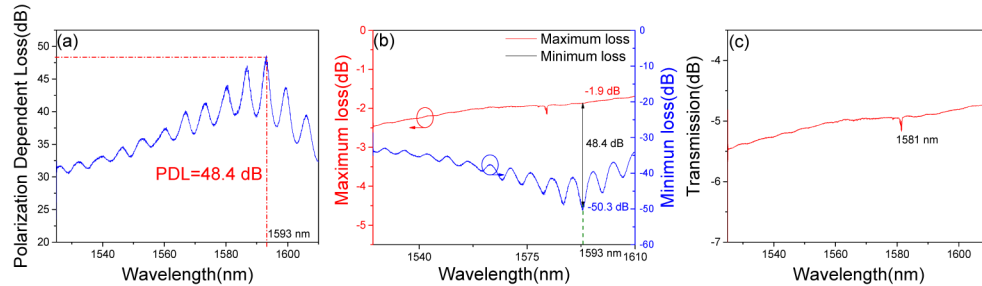

Fig. 1. (a) PDL response of 45°TFG. (b) The maximum loss (red line) and minimum loss (blue line) of 45°TFG. (c) The transmission spectrum of 45°TFG.
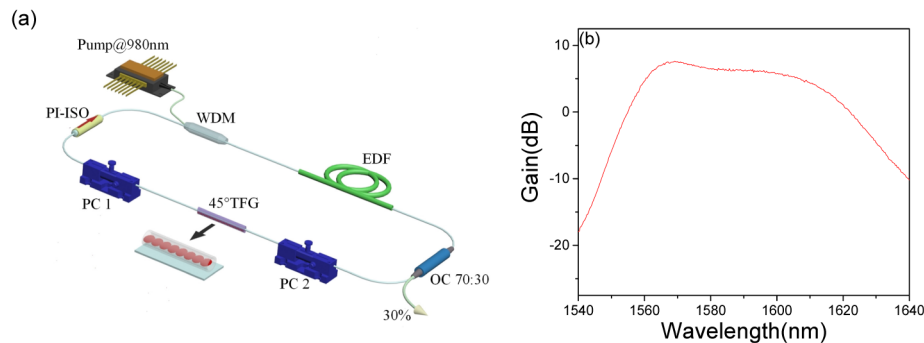

Fig. 2. (a) The configural sketch of wavelength-tunable all-fiber laser using 45°TFG. (b) The gain spectrum of the selected EDF under pump power of 135 mW.

The laser configuration is sketched in Fig. 2. The ring cavity is 9.05 m incorporating a 2.85 m EDF (OFS EDF 80) as gain medium with a group velocity dispersion (GVD) of + 66.1 ps^2/km and 6.05 m SMF with a GVD of −22.8 ps^2/km. The peak absorption of such heavily EDF is 80 dB/m at 1530 nm. It is worth noting that such long highly-doped EDF is chosen intentionally. The corresponding gain spectrum is plotted in Fig. (b). From the picture, we can see that the gain bandwidth is 49 nm, which is from 1560 nm to 1609 nm. Therefore, the highly-doped EDF with optimized length cannot only make the laser work in L-band region, but also provide relatively wide gain bandwidth simultaneously. The pump light at 980 nm is coupled into the cavity through a wavelength-division multiplexer (WDM). To extract 30% laser light, an output coupler (OC) is inserted after the gain medium. In order to prevent intracavity reflection and render the signal light circulate unidirectionally, a polarization-independent isolator (PI-ISO) is employed. And the NPR mechanism is implemented with the combination of the 45°TFG and two polarization controllers (PCs), which can be not only applied as a mode locker but also intended to form intracavity fiber birefringence comb filter. It should be noted that the GVD of 45°TFG is approximately equal to that of SMF. In consequence, the influence of the grating dispersion on mode locking operation is negligible. Also, taking the general conditions of DS into account, the net dispersion is managed to be + 0.05 ps^2.

The characterizations of output pulses are analyzed by an 8 GHz oscilloscope (OSC, KEYSIGHT DSO90804A) and a radio frequency (RF) spectrum analyzer (SIGLENT, SSA

3032X) connecting with a 12.5 GHz high speed photo-detector (PD, Newport 818-BB-51F). The optical spectrum is identified by an optical spectrum analyzer (OSA, Yokogawa AQ6370C) while the pulse duration is measured with an autocorrelator (FEMTOCHROME, FR-103WS).

3. Experimental results and discussions

With suitable polarization state of the laser, the mode locking is obtainable at pump power of 144 mW. Figure 3 shows the performances of output pulses under the pump power of 425 mW. The appearance of near rectangular optical spectral shape with a flat roof and steep sides clearly implies the generation of DSs. This distinct feature of DS results from the spectral filter effect induced by the gain medium and NPR mechanism. As one may notice that the whole spectrum covers L band with central wavelength of 1597.76 nm and 3 dB bandwidth of 26.74 nm. It is postulated that the relatively long highly doped EDF is the key factor to force the laser oscillate at L band, which makes in-band absorption occur [18].The corresponding pulse train is depicted in Fig. 3(b), where the identical pulses exhibit uniform distribution with interval of 43.4 ns which matches well with the cavity length.
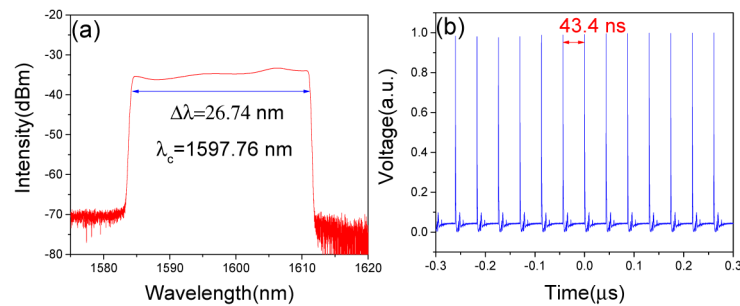

Fig. 3. Pulse performances under pump power of 425 mW (a) Optical spectrum with resolution of 0.02 nm. (b) Pulse train visualized in oscilloscope.

Subsequently, the pump power is increased from 452 mW to 540 mW while the PCs position is fixed. The evolution of optical spectrum is visualized in Fig. 4(a). From the picture, we can see that along with the rise of pump power, the pulses maintain its original spectral shape and the bandwidth of spectrum becomes broader simultaneously, as a typical feature of the DS laser [31,32]. Also, the variations of spectral bandwidth and pulse width versus pump power are plotted in Fig. 4(b). It is found that the 3 dB bandwidth is monotonically increased from 26.74 nm to 31.73 nm while the pulse duration is narrowed down from 20.56 ps to 16.8 ps. The reason is owing to the fact of the enhanced self-phase modulation (SPM) when pump power is increased. The output power, pulse energy and peak power as a function of pump power, are shown in Fig. 4(c) and Fig. 4(d), respectively. Obviously, all of the tendencies are almost linear. And the output power varies from 10.12 mW to 13.02 mW, corresponding to the variations of pulse energy from 0.44 nJ to 0.57 nJ and the peak power from 21.37 W to 33.65 W. The resulting pump efficiency is 2.56%. It should be noted that the DS is apt to transform into noise-like pulse when we increase the pump power further, which is rooted in the peak power clamping effect [33]. However, proper selection of intracavity polarization state can lead the pulse restored into DS again.

In our experiment, the widest optical spectrum with 3dB bandwidth of 34.6 nm is observed under 622 mW, as described in Fig. 5(a). The optical spectral shape is similar to that depicted in Fig. 3(a) while there is a visible sideband at 1574 nm. It is because at this point, the high pulse intensity resulting from relatively large pump power is greater than the threshold value of modulation instability, which induces this type of sideband [34]. In this condition, the pulses exhibit 19.02 mW output power and 0.83 nJ pulse energy. In addition, the pulse duration is 15.38 ps provided that the autocorrelation (AC) trace has a Gaussian

shape, resulting in the peak power of 53.7 W. Also, the calculated time bandwidth product (TBP) is 62.57, reflecting the presence of giant chirp, which is a noticeable attribute of DS. Specifically, an additional section of SMF is spliced out of cavity so as to compress the output pulse. The resultant AC trace is plotted in Fig. 5(b). It turns out that the pulse duration can be dechirped to 772 fs. Obviously, the obtained pulses via the dechirping method is still not transform limited, which is further evidenced by the calculated TBP of 3.14. It is speculated that the uncompensated pulse chirp is attributed to the combined effect of nonlinear chirp and high-order dispersion [35], which expressed by the small pedestal in AC trace. If the grating pair [34] or a large-mode area fiber [36] is utilized externally, the pulse chirp is expected to compensate further. Correspondingly, the peak power of the pulses is increased to 1.07 kW. As presented in Fig. 5(c), the signal noise ratio (SNR) is 62 dB, providing a valid proof of the outstanding pulse stability. Also, the RF spectrum with 1 GHz span indicates the pure single pulse operation.
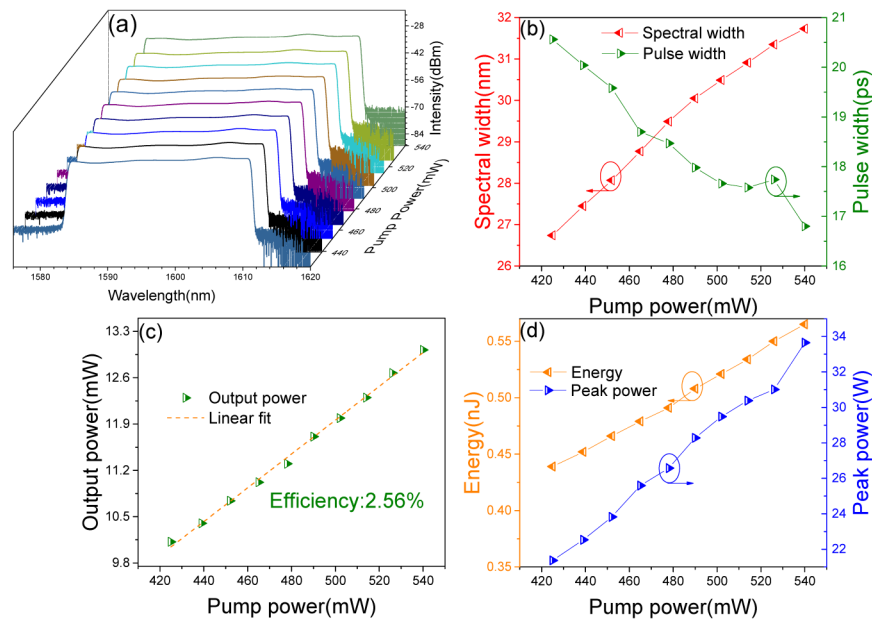

Fig. 4. (a) The evolution of optical spectrum with continuous increasing of pump power from 452 mW to 540 mW. (b) Spectral width and pulse duration versus pump power. (c) The variation of output power against pump power. (c) Pulse energy and peak power as a function of pump power.
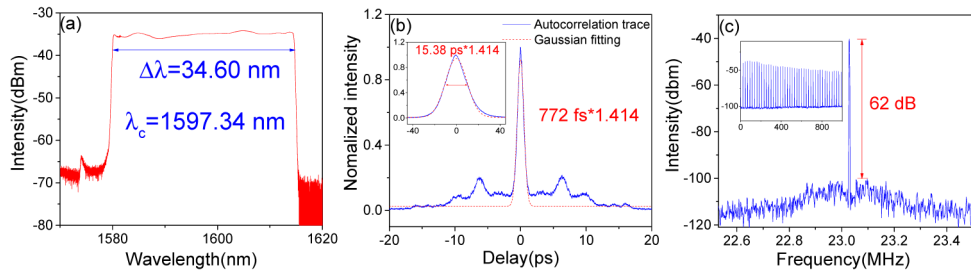

Fig. 5. Typical pulse performances under pump power of 622 mW. (a) Optical spectrum with resolution of 0.02 nm. (b) AC trace of the dechirped pulses. Inset, AC trace of output pulses delivered from cavity directly. (c) RF spectra.

Keeping pump power under 310 mW, the wavelength-tunable operation can be realized easily by merely rotating the PCs carefully and slowly. As illustrated in Fig. 6(a), the center wavelength of obtained DS can be shifted from 1567 nm to 1606 nm, which means that the wavelength-tuning range is 39 nm. To the best of our knowledge, it is the widest spectral-tuning range from which DS fiber laser working in communication band so far. Clearly, all spectra show steep edges, which is a striking feature of DS. Nevertheless, the optical spectral shape changes from quasi-rectangle to rectangle during the wavelength tuning. It is speculated that it mainly results from the different cavity net dispersion and gain intensity under different operating center wavelength. Moreover, the variations of 3dB bandwidth and pulse duration as a function on center wavelength are plotted in Fig. 6(b). It is clear that the 3dB bandwidth varies from 5.5 nm to 21.8 nm while the pulse duration changes from 6.43 ps to 53.9 ps. Obviously, there is no specific relationship between any of them. We attribute it to the variation of intracavity polarization state. The detailed quantitative explanations are as follows. From one hand, the different polarization state can result in the variation of transmission curve versus input power especially the transmission intensity ratio, which changes the modulation depth of the artificial SA [37]. On the other hand, different operating wavelength can make the disparity of gain intensity and dispersion of the laser cavity. All of them affect the pulse evolution, consequently causing different pulse characteristics.
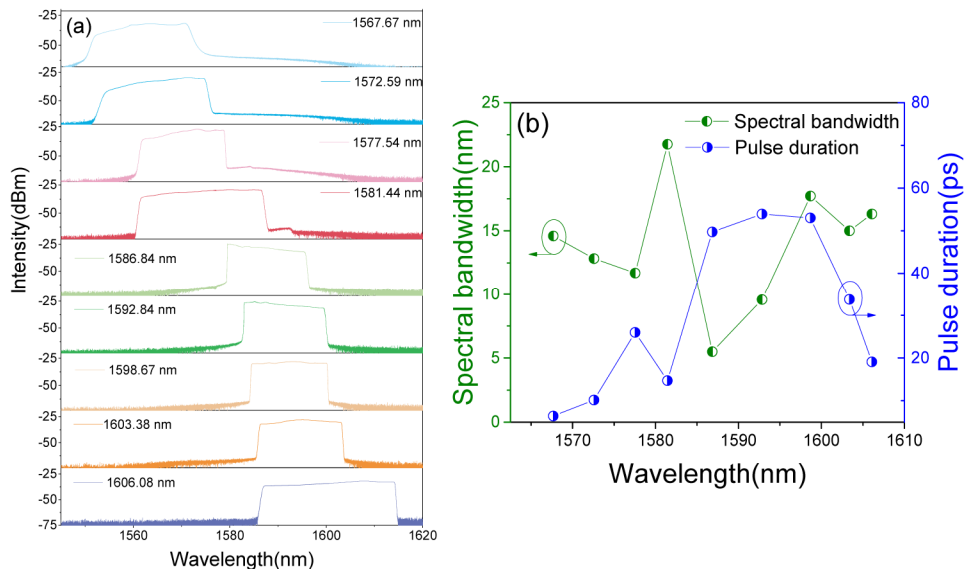

Fig. 6. (a) Optical spectra of tunable wavelength from 1567.67 nm to 1606.08 nm under fixed pump power of 310 mW. (b) Variations of spectral bandwidth and pulse duration as a function on center wavelength.

In particular, the SNR values of pulses at different center wavelengths are illustrated in Fig. 7(a). From the picture, we can see that all SNRs are sustained up to 55 dB, implying that the laser always maintains stable running state regardless the working center wavelength, which is the admirable performance for practical applications. Also, the optical spectrum with center wavelength of 1603 nm is monitored for 8 hours continuously, as presented in Fig. 7(b). It is found that the profile of optical spectra remains constant with barely invisible amplitude fluctuation under laboratory condition, declaring excellent long-term stability.

To our understanding, the wavelength-tunable operation can be interpreted by the NPR-induced intracavity fiber birefringence comb filter. Besides, some previous reports have given the deep impression that rotating PCs can lead to transmission spectrum change for this type filter containing transmission peak position, transmission intensity as well as free spectral

range [20,38,39]. As a result, it alternates the intracavity gain distribution. Since the excited lasing wavelength only occurs at the gain peak location, the wavelength-tunable operation is obtained. Worthy of mentioning, the obtained wavelength-tunable range (39 nm) is much wider than all of the DS fiber lasers operating in C + L band [17,19,20,40,41]. It is believed that the optimizing EDF length plays a great role in the realization of such broad wavelength-tunable range. Because it provides wider gain bandwidth, which satisfies the basic condition of wide wavelength-tunable operation. Also, one may notice that the cavity length is much shorter in comparison with those of most wavelength-tunable fiber lasers [17,19,20,40,41]. Therefore, it is considered that the long cavity length, namely representing large cavity birefringence in our experiment, is not the key factor of realizing widely wavelength-tunable range in fiber laser based on NPR-induced filter. Certainly, it should be guaranteed that the cavity length should be long enough to achieve mode locking with enough nonlinearity. As we know, the bandwidth of NPR-induced filter is determined by intracavity birefringence. The smaller the intracavity birefringence is, the wider bandwidth the NPR-based filter exhibits [20,38,39]. Therefore, in our situation, the relatively short cavity can result in the relatively wide bandwidth of the NPR-induced filter. As such type filter exhibits full operation waveband and rotating PCs can change the peak position of the filter, the wavelength-tunable range will not be affected significantly if the effective gain bandwidth is almost constant. Also, the wide bandwidth of the NPR-induced filter is in favor of realizing wide optical spectrum pulse which is favorable for short pulse duration generation. In our experiment, it is supposed that the spectral-tuning range is limited by the effective gain bandwidth provide by EDF [18,25,26]. It is expected that the broader wavelength-tunable range can be realized if other gain fiber with appropriate length and wider effective gain bandwidth is employed in the cavity such as Er-Yb co-doped fiber [42] and Tm-doped fiber [43].
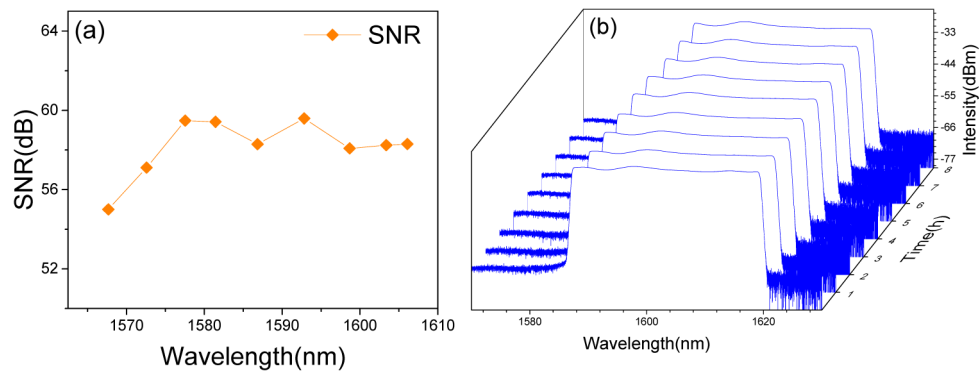

Fig. 7. Spectral tunable DS laser properties: (a) SNR at different center wavelengths. (b) The variation of optical spectra within 8 hours.

4. Conclusions

In conclusion, we experimentally investigated a widely wavelength-tunable L-band all-fiber dissipative soliton Er-doped laser by optimizing the length of EDF. The 45°TFG is incorporated in the laser to be an effective L-band polarizer. Together with two PCs, NPR mechanism is formed, which is used as an artificial saturable absorber as well as intracavity fiber birefringence comb filter. Under pump power of 622 mW, the generated DSs is 15.38 ps centered at 1597.34 nm with 3dB bandwidth of 34.6 nm at 23 MHz. After dechirping the pulses via a section of SMF, the pulse duration is decreased to 772 fs. Interestingly, the wavelength-tunable operation is reflected by the fact that the operating center wavelength of DS can be shifted from 1567 nm to 1606 nm with a range of 39 nm. This is the first demonstration about L-band DS generation from an all-fiber laser using a fiber grating and is

also the widest wavelength-tunable range ever obtained in C + L band DS fiber laser. Especially, emphasis should be given that our cavity length is much shorter than most of conventional wavelength-tunable fiber lasers. Thus, high repetition rate tunable DS fiber laser is feasible. Our experimental results reveal that in fiber laser where the NPR-induced intracavity fiber birefringence comb filter exists, the actual cavity length shows minor influence on the wavelength-tuning range. The demonstrate L-band DS fiber laser not only exhibits short cavity length but also allowing the wide wavelength-tunable operation can be an effective solution for some specific applications in terms of optical communication and material processing.

Funding

References

1. N.-K. Chen, J.-W. Lin, F.-Z. Liu, and S.-K. Liaw, "Wavelength-Tunable Er3+-Doped fs Mode-Locked Fiber Laser Using Short-Pass Edge Filters," IEEE Photonics Technol. Lett. **22**(10), 700–702 (2010).
2. X. Hao, Z. Tong, W. Zhang, and Y. Cao, "A fiber laser temperature sensor based on SMF core-offset structure," Opt. Commun. **335**, 78–81 (2015).
3. Y. W. Lee and B. Lee, "Wavelength-switchable erbium-doped fiber ring laser using spectral polarization-dependent loss element," IEEE Photonics Technol. Lett. **15**(6), 795–797 (2003).
4. Y. Qi, Z. Kang, J. Sun, L. Ma, W. Jin, Y. Lian, and S. Jian, "Wavelength-switchable fiber laser based on few-mode fiber filter with core-offset structure," Opt. Laser Technol. **81**, 26–32 (2016).
5. S. Huang, Y. Wang, P. Yan, J. Zhao, H. Li, and R. Lin, "Tunable and switchable multi-wavelength dissipative soliton generation in a graphene oxide mode-locked Yb-doped fiber laser," Opt. Express **22**(10), 11417–11426 (2014).
6. S. Srivastava, S. Radic, C. Wolf, J. C. Centanni, J. W. Sulhoff, K. Kantor, and Y. Sun, "Ultradense WDM transmission in L-band," IEEE Photonics Technol. Lett. **12**(11), 1570–1572 (2000).
7. J. Zhang, X. Qiao, F. Liu, Y. Weng, R. Wang, Y. Ma, Q. Rong, M. Hu, and Z. Feng, "A tunable erbium-doped fiber laser based on an MZ interferometer and a birefringence fiber filter," J. Opt. **14**(1), 015402 (2012).
8. J. S. Milne, J. M. Dell, A. J. Keating, and L. Faraone, "Widely tunable MEMS-based Fabry–Perot filter," J. Microelectromech. Syst. **18**(4), 905–913 (2009).
9. X. He, Z. B. Liu, and D. N. Wang, "Wavelength-tunable, passively mode-locked fiber laser based on graphene and chirped fiber Bragg grating," Opt. Lett. **37**(12), 2394–2396 (2012).
10. S. H. Yun, I. K. Hwang, and B. Y. Kim, "All-fiber tunable filter and laser based on two-mode fiber," Opt. Lett. **21**(1), 27–29 (1996).
11. J. Wang, A. P. Zhang, Y. H. Shen, H. Y. Tam, and P. K. Wai, "Widely tunable mode-locked fiber laser using carbon nanotube and LPG W-shaped filter," Opt. Lett. **40**(18), 4329–4332 (2015).
12. Z. X. Zhang, Z. W. Xu, and L. Zhang, "Tunable and switchable dual-wavelength dissipative soliton generation in an all-normal-dispersion Yb-doped fiber laser with birefringence fiber filter," Opt. Express **20**(24), 26736–26742 (2012).
13. Z. Yan, X. Li, Y. Tang, P. P. Shum, X. Yu, Y. Zhang, and Q. J. Wang, "Tunable and switchable dual-wavelength Tm-doped mode-locked fiber laser by nonlinear polarization evolution," Opt. Express **23**(4), 4369–4376 (2015).
14. D. Ma, Y. Cai, C. Zhou, W. Zong, L. Chen, and Z. Zhang, "37.4 fs pulse generation in an Er:fiber laser at a 225 MHz repetition rate," Opt. Lett. **35**(17), 2858–2860 (2010).
15. D. Y. Tang and L. M. Zhao, "Generation of 47-fs pulses directly from an erbium-doped fiber laser," Opt. Lett. **32**(1), 41–43 (2007).
16. C. Zou, T. Wang, Z. Yan, Q. Huang, M. Alaraimi, A. Rozhin, and C. Mou, "Wavelength-tunable passively mode-locked Erbium-doped fiber laser based on carbon nanotube and a 45°tilted fiber grating," Opt. Commun. **406**, 151–157 (2018).
17. Z. Wu, S. Fu, C. Chen, M. Tang, P. Shum, and D. Liu, "Dual-state dissipative solitons from an all-normal-dispersion erbium-doped fiber laser: continuous wavelength tuning and multi-wavelength emission," Opt. Lett. **40**(12), 2684–2687 (2015).

18. J. L. Luo, L. Li, Y. Q. Ge, X. X. Jin, D. Y. Tang, D. Y. Shen, S. M. Zhang, and L. M. Zhao, "L-band femtosecond fiber laser mode locked by nonlinear polarization rotation," IEEE Photonics Technol. Lett. **26**(24), 2438–2441 (2014).

19. D. D. Han, "Experimental and theoretical investigations of a tunable dissipative soliton fiber laser," Appl. Opt. **53**(32), 7629–7633 (2014).

20. D. Yan, X. Li, S. Zhang, M. Han, H. Han, and Z. Yang, "L-band wavelength-tunable dissipative soliton fiber laser," Opt. Express **24**(2), 739–748 (2016).

21. L. Nelson, D. Jones, K. Tamura, H. Haus, and E. Ippen, "Ultrashort-pulse fiber ring lasers," Appl. Phys. B **65**(2), 277–294 (1997).

22. D. Tang, L.-M. Zhao, B. Zhao, and A. Liu, "Mechanism of multisoliton formation and soliton energy quantization in passively mode-locked fiber lasers," Phys. Rev. A **72**(4), 043816 (2005).

23. E. Thoen, E. Koontz, M. Joschko, P. Langlois, T. Schibli, F. Kärtner, E. Ippen, and L. Kolodziejski, "Two-photon absorption in semiconductor saturable absorber mirrors," Appl. Phys. Lett. **74**(26), 3927–3929 (1999).

24. L. Wang, X. Liu, Y. Gong, D. Mao, and H. Feng, "Ultra-broadband high-energy pulse generation and evolution in a compact erbium-doped all-fiber laser," Laser Phys. Lett. **8**(5), 376–381 (2011).

25. X. Dong, P. Shum, N. Ngo, C. Chan, B. O. Guan, and H. Y. Tam, "Effects of active fiber length on the tunability of erbium-doped fiber ring lasers," Opt. Express **11**(26), 3622–3627 (2003).

26. Xinyong Dong, P. Shum, N. Q. Ngo, H.-Y. Tam, and Xiaoyi Dong, "Output power characteristics of tunable erbium-doped fiber ring lasers," J. Lightwave Technol. **23**(3), 1334–1341 (2005).

27. K. Zhou, G. Simpson, X. Chen, L. Zhang, and I. Bennion, "High extinction ratio in-fiber polarizers based on 45 ° tilted fiber Bragg gratings," Opt. Lett. **30**(11), 1285–1287 (2005).

28. C. Mou, H. Wang, B. G. Bale, K. Zhou, L. Zhang, and I. Bennion, "All-fiber passively mode-locked femtosecond laser using a 45°-tilted fiber grating polarization element," Opt. Express **18**(18), 18906–18911 (2010).

29. T. Wang, Z. Yan, Q. Huang, C. Zou, C. Mou, K. Zhou, and Z. Lin, "Mode locked Erbium doped fiber lasers using 45° tilted fiber grating," IEEE J. Sel. Top. Quantum Electron. **24**(3), 1101056 (2017).

30. Z. Yan, C. Mou, K. Zhou, X. Chen, and L. Zhang, "UV-Inscription, Polarization-Dependant Loss Characteristics and Applications of 45 °Tilted Fiber Gratings," J. Lightwave Technol. **29**(18), 2715–2724 (2011).

31. A. Cabasse, B. Ortaç, G. Martel, A. Hideur, and J. Limpert, "Dissipative solitons in a passively mode-locked Er-doped fiber with strong normal dispersion," Opt. Express **16**(23), 19322–19329 (2008).

32. Z. Zhang, Z. Yan, K. Zhou, and Z. Lin, "All-fiber 250 MHz fundamental repetition rate pulsed laser with tilted fiber grating polarizer," Laser Phys. Lett. **12**(4), 045102 (2015).

33. L. M. Zhao, D. Y. Tang, J. Wu, X. Q. Fu, and S. C. Wen, "Noise-like pulse in a gain-guided soliton fiber laser," Opt. Express **15**(5), 2145–2150 (2007).

34. D. Y. Tang, L. M. Zhao, X. Wu, and H. Zhang, "Soliton modulation instability in fiber lasers," Phys. Rev. A **80**(80), 2554–2558 (2009).

35. J. Xu, S. Wu, H. Li, J. Liu, R. Sun, F. Tan, Q.-H. Yang, and P. Wang, "Dissipative soliton generation from a graphene oxide mode-locked Er-doped fiber laser," Opt. Express **20**(21), 23653–23658 (2012).

36. X. Li, Y. Wang, W. Zhao, X. Liu, Y. Wang, Y. H. Tsang, W. Zhang, X. Hu, Z. Yang, C. Gao, C. Li, and D. Shen, "All-fiber dissipative solitons evolution in a compact passively Yb-doped mode-locked fiber laser," J. Lightwave Technol. **30**(15), 2502–2507 (2012).

37. W. S. Man, H. Y. Tam, M. S. Demokan, P. K. A. Wai, and D. Y. Tang, "Mechanism of intrinsic wavelength tuning and sideband asymmetry in a passively mode-locked soliton fiber ring laser," J. Opt. Soc. Am. B **17**(1), 28–33 (2000).

38. C. Zou, Q. Huang, T. Wang, Z. Yan, M. AlAraimi, A. Rozhin, and C. Mou, "Single/dual-wavelength switchable bidirectional Q-switched all-fiber laser using a bidirectional fiber polarizer," Opt. Lett. **43**(19), 4819–4822 (2018).

39. H. Zhang, D. Tang, R. Knize, L. Zhao, Q. Bao, and K. P. Loh, "Graphene mode locked, wavelength-tunable, dissipative soliton fiber laser," Appl. Phys. Lett. **96**(11), 111112 (2010).

40. Q. Wang, Y. Chen, L. Miao, G. Jiang, S. Chen, J. Liu, X. Fu, C. Zhao, and H. Zhang, "Wide spectral and wavelength-tunable dissipative soliton fiber laser with topological insulator nano-sheets self-assembly films sandwiched by PMMA polymer," Opt. Express **23**(6), 7681–7693 (2015).

41. Z. Wu, S. Fu, C. Chen, M. Tang, P. Shum, and D. Liu, "Dual-state dissipative solitons from an all-normal-dispersion erbium-doped fiber laser: continuous wavelength tuning and multi-wavelength emission," Opt. Lett. **40**(12), 2684–2687 (2015).

42. Y. Meng, M. Salhi, A. Niang, K. Guesmi, G. Semaan, and F. Sanchez, "Mode-locked Er:Yb-doped double-clad fiber laser with 75-nm tuning range," Opt. Lett. **40**(7), 1153–1156 (2015).

43. K. Yin, B. Zhang, G. Xue, L. Li, and J. Hou, "High-power all-fiber wavelength-tunable thulium doped fiber laser at 2 µm," Opt. Express **22**(17), 19947–19952 (2014).